

Why summation by parts is not enough *

Jan Glaubitz[†], Armin Iske[‡], Joshua Lampert[‡], and Philipp Öffner[§]

Abstract. We investigate the construction and performance of summation-by-parts (SBP) operators, which offer a powerful framework for the systematic development of structure-preserving numerical discretizations of partial differential equations. Previous approaches for the construction of SBP operators have usually relied on either local methods or sparse differentiation matrices, as commonly used in finite difference schemes. However, these methods often impose implicit requirements that are not part of the formal SBP definition. We demonstrate that adherence to the SBP definition alone does not guarantee the desired accuracy, and we identify conditions for SBP operators to achieve both accuracy and stability. Specifically, we analyze the error minimization for an augmented basis, discuss the role of sparsity, and examine the importance of nullspace consistency in the construction of SBP operators. Furthermore, we show how these design criteria can be integrated into a recently proposed optimization-based construction procedure for function space SBP (FSBP) operators on arbitrary grids. Our findings are supported by numerical experiments that illustrate the improved accuracy for the numerical solution using the proposed SBP operators.

Key words. Summation-by-parts operators, general function spaces, initial boundary value problems, stability

AMS subject classifications (2020). 65N12, 65D25

Code repository. https://github.com/JoshuaLampert/2026_SBP_not_enough

DOI. Not yet assigned

1. Introduction. Summation-by-parts (SBP) operators have emerged as a powerful tool in the numerical approximation of partial differential equations (PDEs), particularly conservation laws of the form

$$(1.1) \quad \partial_t \mathbf{u}(t, \mathbf{x}) + \nabla \cdot \mathbf{f}(\mathbf{u}) = 0, \quad t > 0, \quad \mathbf{x} \in \Omega,$$

with conserved variable $\mathbf{u} : \mathbb{R}_{>0} \times \Omega \rightarrow \mathbb{R}^m$, flux function $\mathbf{f} : \mathbb{R}^m \rightarrow \mathbb{R}^{m \times d}$, and $\Omega \subset \mathbb{R}^d$. Conservation laws are fundamental in modeling a wide range of physical phenomena, including fluid dynamics, electromagnetism, and traffic flow. Accurate and stable numerical methods for solving conservation laws are thus crucial for reliable simulations in science and engineering. SBP operators mimic the integration-by-parts property at the discrete level, which is essential for ensuring conservation and stability in numerical schemes. Many classes of discretizations for hyperbolic conservation laws can be formulated in terms of SBP operators, including finite difference (FD) [22, 38, 27], finite volume [29, 30], continuous Galerkin [20, 19, 1], discontinuous Galerkin (DG) [10, 7, 8], radial basis function (RBF) [16], flux reconstruction [35, 31], active flux [3, 2], and overset-grid [14] methods. See also the review articles [9] and [39] for more details.

Traditionally, SBP operators have been constructed based on exactness with respect to polynomial bases. Recently, this has been extended to general finite-dimensional function spaces [15, 12, 17] yielding

*February 12, 2026

Corresponding author: Joshua Lampert

[†]Department of Mathematics, Linköping University, Sweden (jan.glaubitz@liu.se, orcid.org/0000-0002-3434-5563)

[‡]Department of Mathematics, University of Hamburg, Germany (armin.iske@uni-hamburg.de, orcid.org/0000-0003-1743-5484 and joshua.lampert@uni-hamburg.de, orcid.org/0009-0007-0971-6709)

[§]Institute of Mathematics, Clausthal University of Technology, Germany (mail@philippoeffner.de, orcid.org/0000-0002-1367-1917)

function space based SBP (FSBP) operators, which we will build upon to keep the discussion general. In the design of SBP operators, usually different criteria, which go beyond the SBP definition, need to be considered. However, these criteria are not always explicitly stated and generally vary between different applications and discretization methods. Therefore, it is desirable to have an overview of these additional conditions and a general framework for the design of SBP operators that can be tailored to specific applications.

Our contribution. We provide a description and explanation of why the conditions in the definition of SBP operators alone are generally not sufficient for applications to hyperbolic PDEs. To support this observation, we present numerical examples demonstrating the limitations of SBP operators not respecting additional structure. These structures were implicit in previous construction procedures; in this paper we make these requirements explicit and discuss their relevance. Furthermore, we discuss approaches to add additional conditions that make the resulting SBP operators well-suited for solving hyperbolic conservation laws. We investigate two strategies how these can be incorporated into an existing construction procedure. Specifically, we investigate sparsity to construct globally applicable FSBP operators (typically used in FD methods) and regularization techniques to improve accuracy of local FSBP operators (typically used in DG methods). We restrict the discussion to SBP operators in one spatial dimension and use tensor products for higher dimensions.

Outline. Section 2 reviews the theory of SBP operators and existing construction methods. Illustrative examples of SBP operators meeting the standard conditions but failing in practical applications are provided in Section 3, which demonstrates the necessity for additional criteria. Section 4 discusses different strategies to enforce additional structure on SBP operators and how to incorporate these into a recently proposed optimization-based construction method. It also presents numerical experiments demonstrating the effectiveness of the proposed approaches. Finally, Section 5 summarizes the findings and outlines directions for future research.

2. Background. For a set of one-dimensional nodes $X = \{x_i\}_{i=1}^N$, we write $\mathbf{x} = [x_1, \dots, x_N]^T$ and $\mathbf{u} = [u(x_1), \dots, u(x_N)]^T$ for some function u , and $\mathbf{u}' = [u'(x_1), \dots, u'(x_N)]^T$ for its derivative as well as $\mathbf{e}_L = [1, 0, \dots, 0]^T$ and $\mathbf{e}_R = [0, \dots, 0, 1]^T$ for the left and right boundary basis vectors, respectively.

We base our discussion on the recently proposed extension of SBP operators to general finite-dimensional function spaces [15, 16, 17].

Definition 2.1 (FSBP operators). Let $\mathcal{F} \subset C^1([x_L, x_R])$ be a finite-dimensional function space. We say $D = P^{-1}Q$ is an \mathcal{F} -exact FSBP operator, approximating the first derivative operator ∂_x on the node set X , if

- (i) $D\mathbf{f} = \mathbf{f}'$ for all $\mathbf{f} \in \mathcal{F}$,
- (ii) the norm matrix P is symmetric positive definite, and
- (iii) $Q + Q^T = B = \mathbf{e}_R \mathbf{e}_R^T - \mathbf{e}_L \mathbf{e}_L^T$.

The first condition ensures that the derivative is exact on the function space \mathcal{F} . For traditional SBP operators, \mathcal{F} is usually chosen as the space of polynomials up to a certain degree. The second condition ensures that P defines a discrete inner product $\langle \mathbf{u}, \mathbf{v} \rangle_P = \mathbf{u}^T P \mathbf{v}$ approximating $\int_{x_L}^{x_R} uv \, dx$. The third condition is the SBP property, which mimics integration by parts discretely.

SBP operators can be grouped into two classes: (i) dense local operators, which are usually based on collocation and used in finite element (FE) methods and (ii) sparse global operators, which are usually employed in FD methods. This distinction is essential in the design of SBP operators, since the requirements for the two classes differ significantly. Due to the collocation approach, the construction of polynomial SBP operators from the first class is usually straightforward, when restricted to nodes that correspond to a Gaussian quadrature. Examples include Gauss-Lobatto-Legendre operators [10] or

generalized SBP operators based on, e.g., Gauss-Legendre or Gauss-Radau nodes, which do not include one or both boundary points. See [21] for more details.

Classical FD-SBP operators have been constructed for various orders of accuracy and grid configurations, with optimization strategies for the norm and derivative matrices described in [27, 25, 26]. These procedures build upon classical FD approximations and result in derivative matrices D with banded structures and boundary closures. However, these classical FD-SBP operators are limited to polynomial bases and specific grids, which are usually equidistant in the interior.

Recently, an optimization-based procedure for constructing FSBP operators on general node sets and function spaces has been proposed in [17]. The work [17] focused on dense local operators typically applied in FE methods. It formulates the construction of FSBP operators as an optimization problem using only the definition of an SBP operator. Since our construction algorithms presented in this paper are based on this approach, and to set the notation, we briefly summarize the main idea here.

From now on, we focus on diagonal-norm FSBP operators, i.e., P is a diagonal matrix. Let $S = (Q - Q^T)/2$ be the antisymmetric part of Q and let V and V_x be the Vandermonde matrices of a basis $\{f_j\}_{j=1}^K$ of \mathcal{F} and the derivatives $\{f'_j\}_{j=1}^K$ evaluated at X , i.e., $V_{ij} = f_j(x_i)$ and $(V_x)_{ij} = f'_j(x_i)$. The key idea is to rewrite condition (i) from [Definition 2.1](#) as $XW + BV/2 = 0$, where $X = [S, P] \in \mathbb{R}^{N \times 2N}$ is a matrix of the unknowns and $W = [V; -V_x] \in \mathbb{R}^{2N \times K}$ is known. In this setting, $D = P^{-1}(S + B/2)$ being an \mathcal{F} -exact FSBP operator is equivalent to X being a global minimizer of the constrained quadratic optimization problem

$$(2.1) \quad \min_{X \in \mathcal{X}} \|XW + BV/2\|^2$$

with constraints

$$(2.2) \quad \mathcal{X} = \{X = [S, P] \mid S^T = -S, P = \text{diag}(p_1, \dots, p_N), p_i > 0\}$$

and $\|XW + BV/2\| = 0$. The constraints can be removed for diagonal-norm operators by parametrizing P and S by vectors $\boldsymbol{\rho} \in \mathbb{R}^N$ and $\boldsymbol{\sigma} \in \mathbb{R}^L$ as

$$(2.3) \quad P(\boldsymbol{\rho}) = \text{diag}(s(\rho_1), \dots, s(\rho_N)),$$

for the sigmoid logistic function $s(x) = \frac{1}{1+e^{-x}}$, and

$$(2.4) \quad S(\boldsymbol{\sigma}) = \begin{pmatrix} 0 & \sigma_1 & \sigma_2 & \sigma_3 & \dots & \sigma_{N-1} \\ -\sigma_1 & 0 & \sigma_N & \sigma_{N+1} & \dots & \sigma_{2N-3} \\ -\sigma_2 & -\sigma_N & 0 & \sigma_{2N-2} & \dots & \sigma_{3N-6} \\ \vdots & \vdots & \vdots & \ddots & \vdots & \vdots \\ -\sigma_{N-2} & -\sigma_{2N-4} & -\sigma_{3N-7} & -\sigma_{4N-11} & \ddots & \sigma_L \\ -\sigma_{N-1} & -\sigma_{2N-3} & -\sigma_{3N-6} & -\sigma_{4N-10} & \dots & 0 \end{pmatrix} \in \mathbb{R}^{N \times N},$$

where $L = N(N - 1)/2$. The sigmoid function ensures that the positivity constraint $p_i > 0$ is automatically satisfied. Substituting (2.3) and (2.4) into (2.1) yields the unconstrained optimization problem

$$(2.5) \quad \min_{\boldsymbol{\rho} \in \mathbb{R}^N, \boldsymbol{\sigma} \in \mathbb{R}^L} \|X(\boldsymbol{\rho}, \boldsymbol{\sigma})W + BV/2\|^2.$$

In principle, any matrix norm can be used as all norms are equivalent in a finite-dimensional vector space. In our computational examples, we use the Frobenius norm.

Remark 2.2. To solve the optimization problem, we employ the Julia [6] package Optim.jl [28]. We use the limited memory Broyden–Fletcher–Goldfarb–Shanno (LBFGS) algorithm, which needs the gradient of the optimization function, but, in contrast to the Newton method, uses an approximation of the Hessian matrix. We use automatic differentiation (AD) to compute the gradient. Note that the unconstrained optimization problem is not convex, which means that—in theory—the minimum might not be unique and the LBFGS algorithm might not converge to a global minimum. However, in our experiments this was usually no problem and using global solvers for non-convex problems or solving the (convex) constrained problem did not yield any better results and were usually less efficient. A more detailed analysis is of interest, but is left for future work.

Note that the above construction procedure is general and can be used to construct FSBP operators for arbitrary node sets and function spaces. However, generally, no additional properties are enforced on the resulting operators, which are often necessary in practical applications. Examples, where this is problematic, are presented in the next section.

3. Counterexample of FSBP operators. To motivate the need for additional conditions on SBP operators beyond those specified in [Definition 2.1](#), we present some illustrative examples of SBP operators that satisfy the standard SBP conditions but exhibit undesirable properties.

Example 3.1. Consider the extreme case, where the differentiation matrix D has rank one and the mass matrix P is nearly singular:

$$(3.1) \quad D = \begin{pmatrix} -1 & 0 & \dots & 0 & 1 \\ -1 & 0 & \dots & 0 & 1 \\ \vdots & \vdots & \vdots & \vdots & \vdots \\ -1 & 0 & \dots & 0 & 1 \\ -1 & 0 & \dots & 0 & 1 \end{pmatrix}, \quad P = \frac{1}{2} \operatorname{diag}(1, \varepsilon, \dots, \varepsilon, 1).$$

The above operator defined by D and P on $X = \{(i-1)/(N-1)\}_{i=1,\dots,N}$ can get arbitrarily close to an SBP operator for $\mathcal{F} = \operatorname{span}\{1, x\}$ when $\varepsilon \rightarrow 0$. Although this operator numerically is a valid solution to the optimization problem [\(2.1\)](#)–[\(2.2\)](#), it is evident that the differentiation matrix is not a suitable discrete derivative in a non-periodic domain as it only uses information from the boundary nodes.

In the following, we present numerical demonstrations of SBP operators, which are exact for higher-order polynomials, but still fail to accurately solve the linear advection equation

$$(3.2) \quad \partial_t u + a \partial_x u = 0, \quad t \in [0, 1.75], \quad x \in [-1, 1],$$

even for smooth solutions. To this end, we construct global FSBP operators using the optimization-based approach described in [Section 2](#) for polynomial bases $\mathcal{F} = \operatorname{span}\{x^i, i = 0, \dots, d\}$ of different degrees d on $N = 50$ equidistant nodes. As the initial condition, we use $u_0(x) = \sin(k\pi x)$, set the advection velocity to $a = 2$, and use different values for k . The spatial discretization is combined with a third-order strong-stability-preserving Runge–Kutta method with five stages [18]. We use a CFL number of 0.5 for time integration. The results are shown in [Figure 1](#) for $k = 1$ (left) and $k = 2$ (right). It can be observed that the numerical solution using the FSBP operators with polynomial degrees $d \leq 3$ is highly inaccurate, despite the fact that these SBP operators are exact for polynomials of degree up to d . This is especially the case for increasing frequency in the initial condition, where even high-order FSBP operators yield inaccurate results. This suggests that underresolved modes are not sufficiently damped. Note that all numerical solutions are conservative up to machine precision and energy-stable

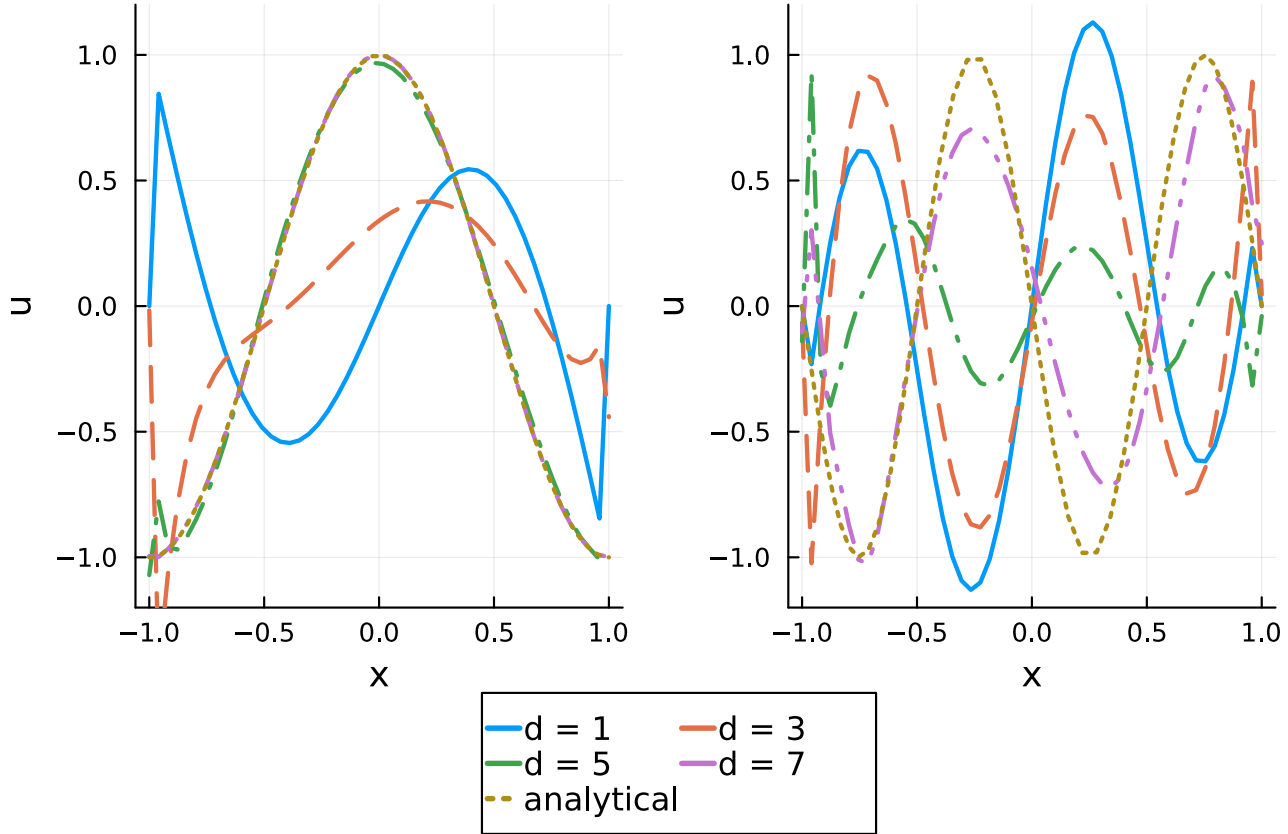


Figure 1: Numerical solutions of the linear advection equation using FSBP operators with different polynomial degrees d on $N = 50$ nodes and at $t = 1.75$. The left subplot shows the solution for $k = 1$ and the right subplot for $k = 2$ in the initial condition $u_0(x) = \sin(k\pi x)$.

Table 1: L^2 - and L^∞ -errors for FSBP and FD-SBP operators with different degrees/orders for the linear advection equation with $N = 50$ nodes, $k = 1$, and $t = 1.75$.

Error	FSBP						Classical FD		
	$d = 1$	$d = 3$	$d = 5$	$d = 7$	$d = 9$	$d = 11$	$p = 2$	$p = 4$	$p = 6$
L^2	8.3e-01	4.7e-01	3.9e-02	1.9e-03	6.6e-05	2.1e-05	2.1e-02	3.2e-04	1.4e-04
L^∞	1.8e+00	9.8e-01	2.1e-01	6.8e-03	2.2e-04	3.2e-05	3.1e-02	5.8e-04	3.6e-04

due to the SBP property and the inclusion of constants in the function space [15]. This implies that energy stability alone is not sufficient to ensure accurate results.

The discrete L^2 - and L^∞ -errors for the different operators are summarized in Table 1 for $k = 1$. As a comparison, we also include the errors using a classical fourth-order FD-SBP operator with a diagonal norm and standard boundary closures [27]. Noticeable, the SBP operators constructed by the optimization procedure yield more accurate results for larger bases including polynomials up to degree $d = 9$ or $d = 11$. The highest degree for which the optimization converges to a minimum with zero

residual in this setup was $d = 12$. It is worth mentioning that the optimization problem is usually not significantly harder to solve for larger bases, and the computation time depends more on the number of nodes N than on the basis size. Typically, larger bases need some more iterations to converge. We observed similar results for other function spaces, e.g., exponential, trigonometric, and radial basis functions. We omit these results here for brevity.

4. Enforcing additional structure of FSBP operators. As demonstrated in the previous section, SBP operators that satisfy the standard conditions from [Definition 2.1](#) are not necessarily well-suited for practical applications, e.g., numerically solving hyperbolic PDEs. This raises the question: What additional properties should an SBP operator have to ensure accurate approximation of derivatives and integrals? The previous section illustrated that unresolved modes can lead to inaccurate solutions. Unresolved modes are connected to functions, which are not correctly differentiated by the SBP operator. A subclass of unresolved modes are nullmodes, i.e., non-constant functions mapped to zero by the differentiation matrix. This suggests that the nullspace of the differentiation matrix,

$$(4.1) \quad \text{null}(D) = \{\mathbf{u} \in \mathbb{R}^N : D\mathbf{u} = 0\},$$

plays a crucial role. Since the differentiation matrix should approximate the first derivative operator, it is natural to require that its nullspace only contains constant functions, i.e., $\text{null}(D) = \text{span}\{1\}$. Such SBP operators are called *nullspace consistent* [\[40, 33, 24, 23, 42, 13, 3\]](#). The importance of nullspace consistency has been highlighted in [\[40\]](#), where it was proven that it is a necessary condition for convergence of SBP schemes. Since we always include the constant function in the function space \mathcal{F} to ensure conservation [\[15\]](#), the SBP operator is *consistent* and problems can only arise from non-constant elements in the nullspace. A useful and easy-to-verify characterization of nullspace consistency is given by the following lemma.

Lemma 4.1. *A consistent SBP operator is nullspace consistent if and only if $\text{rank}(D) = N - 1$.*

Proof. Since the SBP operator is consistent, we have $1 \in \text{null}(D)$ and thus $\dim(\text{null}(D)) \geq 1$. By the rank-nullity theorem, we have $\dim(\text{null}(D)) + \text{rank}(D) = N$. Therefore, $\text{null}(D) = \text{span}\{1\}$ is equivalent to $\dim(\text{null}(D)) = 1$ and thus to $\text{rank}(D) = N - 1$. \blacksquare

Another useful characterization of nullspace consistency is given in [\[23\]](#).

Lemma 4.2. *An SBP operator $D = P^{-1}(S + B/2)$ is nullspace consistent if and only if the matrix*

$$(4.2) \quad \tilde{D} = D + \nu P^{-1} \mathbf{e}_L \mathbf{e}_L^T$$

is invertible for some $\nu \neq 0$.

Proof. See [\[23, Lemma 1\]](#). \blacksquare

It is known that nullspace consistency is not automatically guaranteed by the SBP conditions and explicit counterexamples are presented in [\[40, 24, 23\]](#). In many cases an even stronger property than nullspace consistency, the *eigenvalue property* [\[23\]](#), is necessary, which states that all eigenvalues of \tilde{D} in [\(4.2\)](#) have positive real part for any $\nu > 1/2$.

Coming back to the examples from [Section 3](#), we observe that the dense FSBP operators constructed there have ranks significantly smaller than $N - 1$ ranging from 3 for $d = 1$ to 25 for $d = 11$ (with $N = 50$). Analogously, the eigenvalue property is not satisfied for these operators with the number of eigenvalues with non-positive real parts of \tilde{D} usually being $\text{rank}(D)$ or $\text{rank}(D) + 1$. This indicates that many nullmodes exist, which can explain the poor performance, especially for higher frequencies.

Remark 4.3. An approach to avoid undesirable nullmodes and thus ensuring nullspace consistency for FSBP operators is to enforce the eigenvalue property during the construction of FSBP operators by including an additional constraint in the optimization problem (2.5), yielding

$$(4.3) \quad \begin{aligned} & \min_{\sigma \in \mathbb{R}^N, \rho \in \mathbb{R}^L} \|X(\sigma, \rho)W + BV/2\|^2 \quad \text{s.t.} \\ & \Re(\lambda) > 0 \quad \text{for all } \lambda \in \text{spec} \left(P(\rho)^{-1}(S(\sigma) + B/2) + \nu P(\rho)^{-1} \mathbf{e}_L \mathbf{e}_L^T \right), \end{aligned}$$

where $\nu > 1/2$ is a fixed parameter, $\Re(\lambda)$ is the real part of the eigenvalue λ , and spec denotes the spectrum of a matrix. Notably, $D = P^{-1}(S + B/2)$ and the constraint thus ensure the eigenvalue property and hence also nullspace consistency. However, directly enforcing a condition on the eigenvalues in an optimization problem is significantly more challenging. That is why we consider two alternative approaches and discuss their impact on the nullspaces of the resulting FSBP operators.

All numerical examples in this section use Trixi.jl [36, 37] for solving the hyperbolic PDEs and SummationByPartsOperatorsExtra.jl¹ for constructing and applying the SBP operators using the framework of SummationByPartsOperators.jl [34]. For the time integration, we use error-based adaptive explicit Runge-Kutta methods from OrdinaryDiffEq.jl [32] with a relative and absolute tolerance of 10^{-14} for the convergence tests and 10^{-6} for the other examples. All examples are reproducible using the code provided in our reproducibility repository [11].

4.1. Using sparse differentiation matrices. By defining the skew-symmetric part S of the differentiation matrix as in (2.4), the resulting differentiation matrix D will generally be dense. This can be desirable in some cases, e.g., because the accuracy is not reduced at the boundaries. However, dense differentiation matrices are typically applied locally. Here, we consider how sparsity can be integrated into the optimization-based construction procedure to obtain FSBP operators, which are applicable globally or on larger blocks. Such operators are used, for instance, in global and multi-block FD methods as well as in spectral schemes. Sparsity is a natural property for global differentiation matrices since derivatives act locally and, as we will see below, it can promote nullspace consistency and thus greatly enhance accuracy. Additionally, it improves performance of both the optimization problem, due to significantly fewer degrees of freedom. Furthermore, the application of the operator becomes more efficient due to optimized computations, e.g. for matrix-vector products. Therefore, it is of interest to enforce a special structure on the differentiation matrix as it is also the case for many classical polynomial-based SBP operators. This structure can be formulated as a block-matrix with sub-blocks in the upper left and lower right corners accounting for the boundaries and a banded structure in the interior [27]. We can enforce this structure within the optimization procedure by adding additional constraints such that, instead of (2.4), S is written as

$$(4.4) \quad S(\sigma) = \begin{pmatrix} M_1 & C_1 & 0 \\ -C_1^T & A & C_2 \\ 0 & -C_2^T & M_2 \end{pmatrix} \in \mathbb{R}^{N \times N}.$$

¹<https://github.com/JoshuaLampert/SummationByPartsOperatorsExtra.jl>

With a bandwidth of b in the interior and a boundary matrix size $c \geq b$ (e.g., $c = 2b$), we have $M_1(\sigma) \in \mathbb{R}^{c \times c}$ and $M_2(\sigma) \in \mathbb{R}^{c \times c}$ being skew-symmetric matrices (of the form (2.4)),

$$(4.5) \quad A(\sigma) = \begin{pmatrix} 0 & \dots & * & & & & \\ \vdots & \ddots & \vdots & \ddots & & & \\ * & \dots & 0 & \dots & * & & \\ & \ddots & \vdots & \ddots & \ddots & \ddots & \\ & & * & \dots & 0 & \dots & * \\ & & & \ddots & \vdots & \ddots & \vdots \\ & & & & * & \dots & 0 \end{pmatrix} \in \mathbb{R}^{(N-2c) \times (N-2c)},$$

and

$$(4.6) \quad C_1(\sigma) = \begin{pmatrix} 0 & 0 \\ \tilde{C}_1 & 0 \end{pmatrix} \in \mathbb{R}^{c \times (N-2c)},$$

where the first block column is of size b and the second of size $N - 2c - b$ as well as

$$(4.7) \quad \tilde{C}_1(\sigma) = \begin{pmatrix} * & & & \\ * & * & & \\ \vdots & \ddots & \ddots & \\ * & \dots & \dots & * \end{pmatrix} \in \mathbb{R}^{b \times b}.$$

The structure for C_2 is the same as for C_1^T . Here, every asterisk represents one potentially non-zero element while respecting the anti-symmetry. In summary, we have two times $c(c-1)/2$ unknowns from M_1 and M_2 , two times $b(b+1)/2$ unknowns from C_1 and C_2 , and $b(N-2c-b) + b(b-1)/2$ unknowns from A resulting in a total of $\tilde{L} = Nb + b(b+1)/2 + c^2 - 2bc - c$ unknowns in the optimization problem for the differentiation matrix. That is, we reduce the number of variables from $L = \mathcal{O}(N^2)$ to $\tilde{L} = \mathcal{O}(Nb)$. Note that for the construction in (4.4)–(4.7) we need $N \geq 2c + b$.

In addition, classical FD-SBP operators with equidistant points in the interior have repeating stencils in A . Moreover, we have $C_2 = \tilde{C}_1$ and $M_2 = \tilde{M}_1$, where the bar $\bar{\cdot}$ denotes permutation of rows and columns. By this approach, we reduce the number of unknowns further to $c(c-1)/2 + b$ variables. Since we are interested in a framework with general (i.e., non-equidistant) nodes and general bases (i.e., not translation-invariant), we allow the more general structure of non-repeating stencils. In our reproducibility repository [11], we provide two numerical examples, which corroborate that for non-equidistant nodes with polynomial bases and for equidistant nodes with RBF bases the optimization problem converges only for non-repeating stencils.

Remark 4.4. The optimization-based construction framework is formulated in a general setting, which allows general sets of points and general bases, but it can also be used to reconstruct classical SBP operators. For instance, we have been able to reconstruct dense Gauß-Lobatto-Legendre operators and classical sparse FD-SBP operators by choosing appropriate nodes, bases, and structures for D . This includes the SBP operators from [27, 25, 26] and shows that our framework extends the existing polynomial-based one by being able to recover it for specific choices, while at the same time being able to generate more general SBP operators for other node distributions and bases.

In the following, we use the sparsity-enforcing approach to construct sparse FSBP operators and use them to solve hyperbolic PDEs. First, we consider a global operator on $N = 50$ equidistant points and

Table 2: L^2 - and L^∞ -errors for FSBP operators with different bandwidths b for the linear advection equation with $N = 50$ nodes, $k = 2$, and $t = 1.75$ using a polynomial function space $\mathcal{P}_2 = \text{span}\{1, x, x^2\}$ and a trigonometric function space $\mathcal{T} = \text{span}\{1, x, \sin(\pi x), \cos(\pi x)\}$.

Error	FSBP with $\mathcal{F} = \mathcal{P}_2$					FSBP with $\mathcal{F} = \mathcal{T}$				
	$b = 3$	$b = 4$	$b = 5$	$b = 6$	dense	$b = 3$	$b = 4$	$b = 5$	$b = 6$	dense
L^2	2.6e-02	7.0e-02	1.4e-01	2.5e-01	1.3e+00	1.2e-03	1.1e-02	2.1e-02	4.5e-02	1.2e+00
L^∞	6.6e-02	1.6e-01	2.9e-01	5.1e-01	2.1e+00	4.1e-03	2.3e-02	4.7e-02	9.7e-02	1.8e+00

apply it to the example from [Section 3](#). We use the polynomial basis $\mathcal{P}_2 = \text{span}\{1, x, x^2\}$ and the basis $\mathcal{T} = \text{span}\{1, x, \sin(\pi x), \cos(\pi x)\}$ with different bandwidths $b = 3, 4, 5, 6$ and $c = 2b$ and compare the resulting operators to the dense operators. Note that for \mathcal{P}_2 and $b = 2$, we would recover the classical fourth order FD-SBP operator, but the optimization procedure does not yield an FSBP operator on \mathcal{T} for a bandwidth of 2. We observe empirically that for polynomial bases \mathcal{P}_d , the smallest bandwidth for which the optimization problem converges successfully is $b = d$, which results in the $2d$ -th order FD-SBP operator. As expected, the results improve significantly compared to the dense operators as shown in [Table 2](#) and smaller bandwidths yield better accuracy.

The most important advantage of the optimization-based construction is its ability to yield FSBP operators on arbitrary finite-dimensional function spaces, which can yield better results than polynomial bases [\[15, 16, 17\]](#). In the above example, using the trigonometric basis \mathcal{T} improves the accuracy compared to the polynomial basis up to degree 2 for all bandwidths. In the case of $k = 1$, where the analytical solution is given by $\sin(\pi(x - at))$, the error for the FSBP operator with the trigonometric basis is purely given by the time integration error (up to solver tolerances) since the solution is exactly represented by the function space.

We also compare sparse and dense operators in a multiblock setting with 8 blocks and $N = 15$ nodes per block for the initial condition $u_0(x) = \exp(-x^2/0.1)$ using \mathcal{P}_3 and \mathcal{T} as basis on equidistant nodes. For the sparse operators, we choose a bandwidth of $b = 3$ and $c = 2b$. The results in [Figure 2](#) show that the sparse operators outperform the dense ones for both bases.

Finally, we use the same sparse and dense FSBP operators in a tensor product setting on the domain $[-1, 1]^2$ to solve the two-dimensional compressible Euler equations

$$(4.8) \quad \frac{\partial}{\partial t} \begin{pmatrix} \rho \\ \rho v_1 \\ \rho v_2 \\ \rho e \end{pmatrix} + \frac{\partial}{\partial x} \begin{pmatrix} \rho v_1 \\ \rho v_1^2 + p \\ \rho v_1 v_2 \\ (\rho e + p)v_1 \end{pmatrix} + \frac{\partial}{\partial x} \begin{pmatrix} \rho v_2 \\ \rho v_1 v_2 \\ \rho v_2^2 + p \\ (\rho e + p)v_2 \end{pmatrix} = \begin{pmatrix} s_1 \\ s_2 \\ s_3 \\ s_4 \end{pmatrix},$$

where $p = (\gamma - 1)(\rho e - \rho(v_1^2 + v_2^2)/2)$ denotes the pressure, ρ the density, v_1 and v_2 the velocities in the x and y directions, e the specific total energy, and γ the ratio of specific heats. We choose $\gamma = 1.4$, periodic boundary conditions, and the manufactured solution

$$(4.9) \quad \begin{aligned} \rho(\mathbf{x}, t) &= c + A \sin(\omega(x_1 + x_2 - t)), & (\rho v_1)(\mathbf{x}, t) &= \rho(\mathbf{x}, t), \\ (\rho v_2)(\mathbf{x}, t) &= \rho(\mathbf{x}, t), & (\rho e)(\mathbf{x}, t) &= \rho(\mathbf{x}, t)^2. \end{aligned}$$

Here, the initial condition is given by the above expression at $t = 0$ and a source term $\mathbf{s} = (s_1, s_2, s_3, s_4)^T$ is added to the equations to ensure that the manufactured solution is an exact solution of the resulting

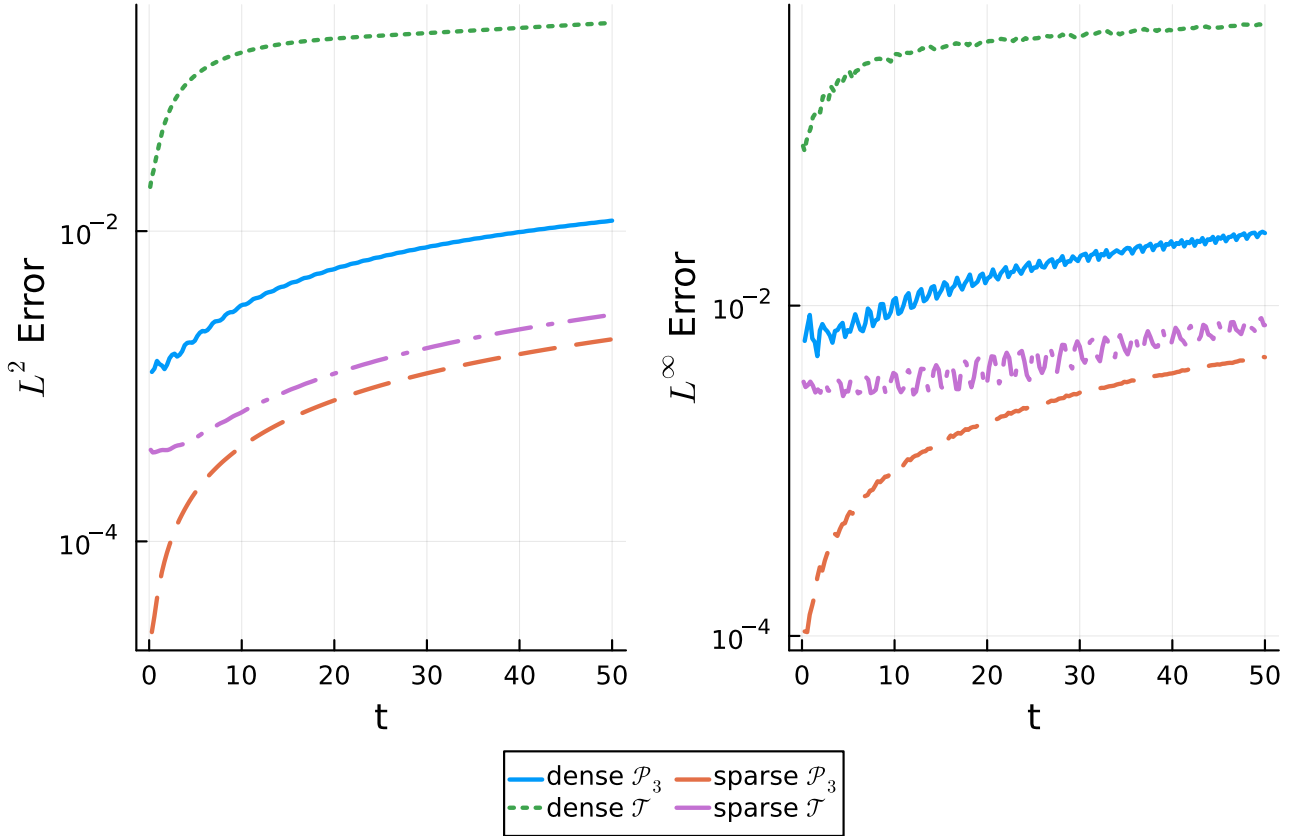


Figure 2: L^2 - and L^∞ -errors for the one-dimensional linear advection equation using FSBP operators based on $\mathcal{P}_3 = \text{span}\{1, x, x^2, x^3\}$ and $\mathcal{T} = \text{span}\{1, x, \sin(\pi x), \cos(\pi x)\}$ on 8 blocks with $N = 15$ nodes per block. Sparse operators with bandwidth $b = 3$ are compared to dense operators.

PDE. For the numerical flux, we choose the HLLC flux [41]. The L^2 - and L^∞ -errors summed across all variables are shown for $c = 2$, $A = 0.1$, $\omega = \pi$ in Figure 3, where we use global operators with $N = 50$ equidistant nodes. Again, the sparse operators outperform the dense ones for both bases. The dense operator for \mathcal{P}_3 crashes after around $t = 4$.

In Table 3 we show L^2 -errors and experimental orders of convergence (EOCs) in the density for the compressible Euler equations using sparse FSBP operators based on \mathcal{P}_3 and \mathcal{T} . The results confirm that high-order convergence is achieved for both bases.

We remark that the dense operators for \mathcal{P}_3 and \mathcal{T} have a rank of 8 each, and are thus not nullspace consistent. At the same time, all sparse operators constructed in this section are numerically nullspace consistent with a rank of $N - 1$.

4.2. Minimizing the error for augmented basis. Two strategies to increase the efficiency of FSBP operators are (i) keeping the basis fixed and optimizing the node locations or minimizing the number of nodes or (ii) enlarging the basis, while keeping the nodes fixed. Inspired by the observation from the Section 3 that FSBP operators can become more accurate when enlarging the basis, here we follow the idea to promote accuracy for functions that are not included in the basis. We consider the case of an FSBP operator on \mathcal{F} for which we want to increase the accuracy by enlarging the basis by another

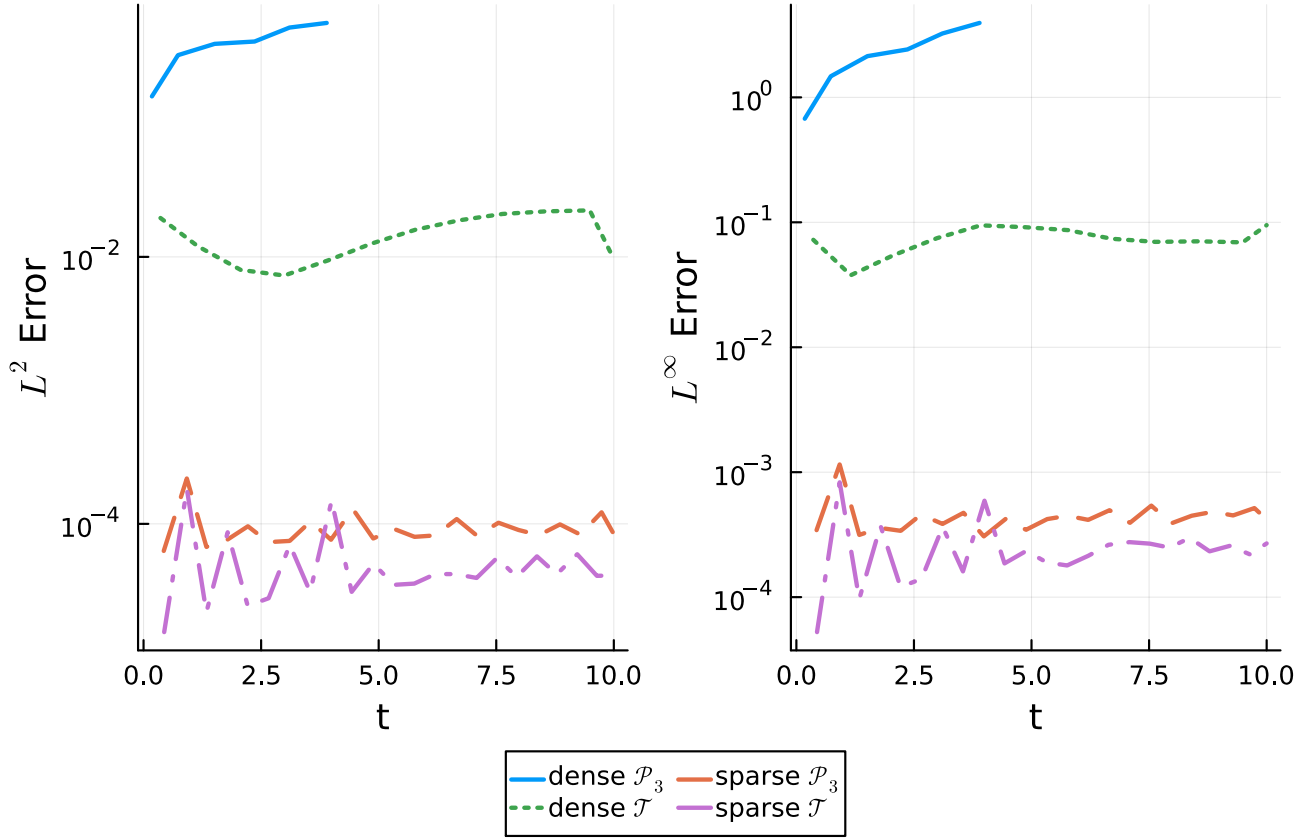


Figure 3: L^2 - and L^∞ -errors summed across all variables for the two-dimensional compressible Euler equations using FSBP operators based on $\mathcal{P}_3 = \text{span}\{1, x, x^2, x^3\}$ and $\mathcal{T} = \text{span}\{1, x, \sin(\pi x), \cos(\pi x)\}$ with global operators on $N = 50$ equidistant nodes. Sparse operators with bandwidth $b = 3$ are compared to dense operators.

Table 3: L^2 -errors and EOCs for the compressible Euler equations and function spaces $\mathcal{F} = \mathcal{P}_3$ and $\mathcal{F} = \mathcal{T}$ using sparse FSBP operators with bandwidth $b = 3$ on K blocks with $N = 15$ nodes each.

(a) $\mathcal{F} = \mathcal{P}_3$						(b) $\mathcal{F} = \mathcal{T}$					
K	ρ	ρv_1	ρv_2	ρe	EOC	K	ρ	ρv_1	ρv_2	ρe	EOC
2	1.82e-04	1.67e-04	1.67e-04	4.61e-04	—	2	7.31e-04	6.99e-04	6.99e-04	1.46e-03	—
4	8.75e-06	9.75e-06	9.75e-06	2.54e-05	4.38	4	1.31e-04	1.30e-04	1.30e-04	4.78e-04	2.48
8	6.23e-07	6.39e-07	6.39e-07	1.75e-06	3.81	8	3.05e-05	3.08e-05	3.08e-05	1.16e-04	2.11
16	6.19e-08	5.63e-08	5.63e-08	1.38e-07	3.33	16	6.41e-06	6.41e-06	6.41e-06	2.50e-05	2.25

set of functions $\mathcal{G} = \{g_1, \dots, g_M\}$. However, there might not exist an FSBP operator that is exact on $\mathcal{F} \cup \text{span}(\mathcal{G})$ on the given set of nodes X . Therefore, we cannot ensure exactness on \mathcal{G} . Instead, we thus minimize the error on \mathcal{G} , which corresponds to solving a regularized optimization problem. We can interpret \mathcal{G} as a set of previously unresolved modes, which are better controlled if we additionally

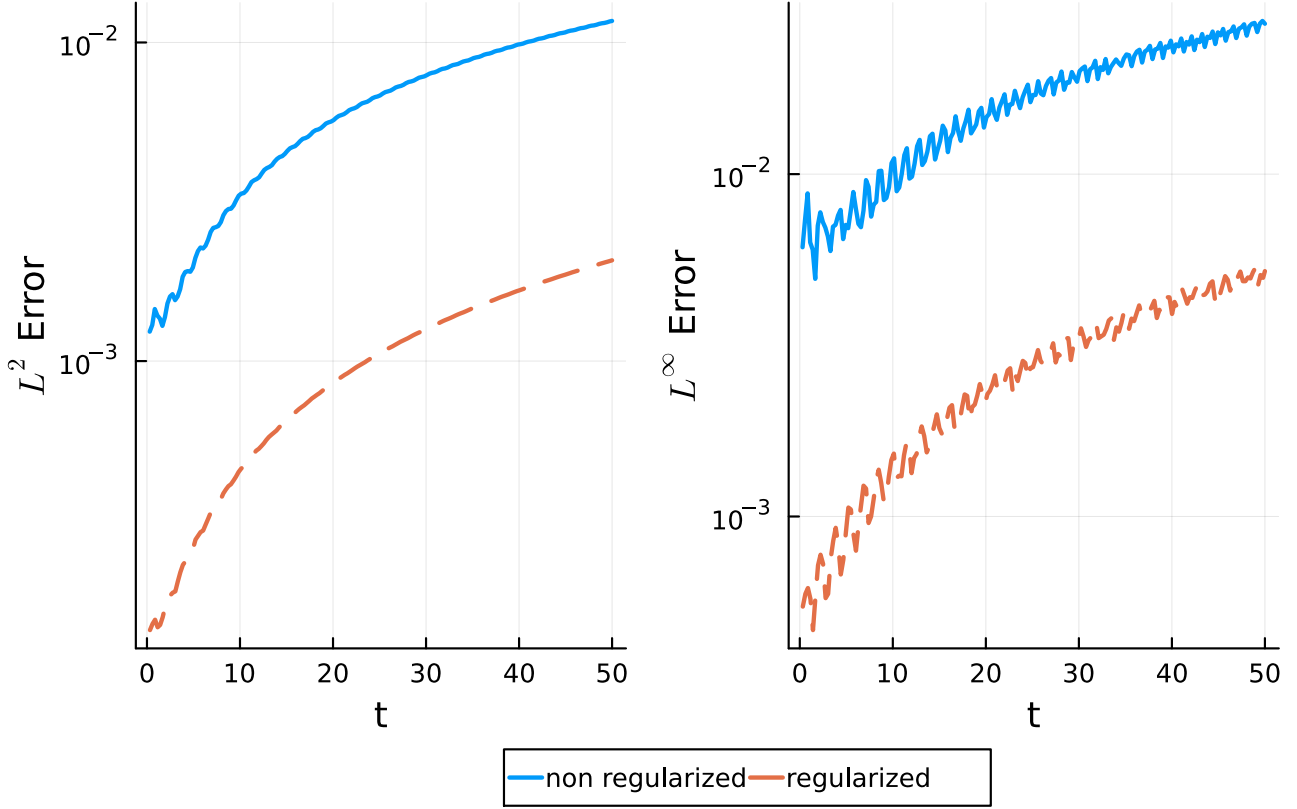


Figure 4: L^2 - and L^∞ -errors for the one-dimensional linear advection equation using FSBP operators based on $\mathcal{P}_3 = \text{span}\{1, x, x^2, x^3\}$ without regularization and with regularization on $\mathcal{G} = \{\sin(\pi x), \cos(\pi x)\}$ on 8 blocks with $N = 15$ nodes per block.

minimize their error. More precisely, instead of solving the optimization problem from (2.1), we solve

$$(4.10) \quad \min_{X \in \mathcal{X}} \|XW + BV/2\|^2 + \sum_{k=1}^M \lambda_k \|D\mathbf{g}_k - \mathbf{g}'_k\|^2$$

for some augmented basis $\mathcal{G} = \{g_1, \dots, g_M\}$ and weights $\lambda_k > 0$. The idea to minimize the error of an SBP operator for higher-order polynomials has also been employed in [26] to construct polynomial FD-SBP operators. In the regularized formulation, we cannot aim for the objective function to become zero, and thus cannot guarantee exactness on \mathcal{F} . This would especially affect conservation since the constant function 1 is usually included in \mathcal{F} and needs to be differentiated exactly by an SBP operator to ensure conservation. To avoid these potential shortcomings of (4.10), we instead formulate the first term in (4.10) as a constraint and minimize the error on \mathcal{G} only:

$$(4.11) \quad \min_{X \in \mathcal{X}} \sum_{k=1}^M \lambda_k \|D\mathbf{g}_k - \mathbf{g}'_k\|^2 \quad \text{s.t.} \quad \|XW + BV/2\|^2 = 0.$$

To demonstrate the potential of this approach, we again consider the one-dimensional linear advection equation with the initial condition given by $u_0(x) = \exp(-x^2/0.1)$ on $[-1, 1]$ and the two-

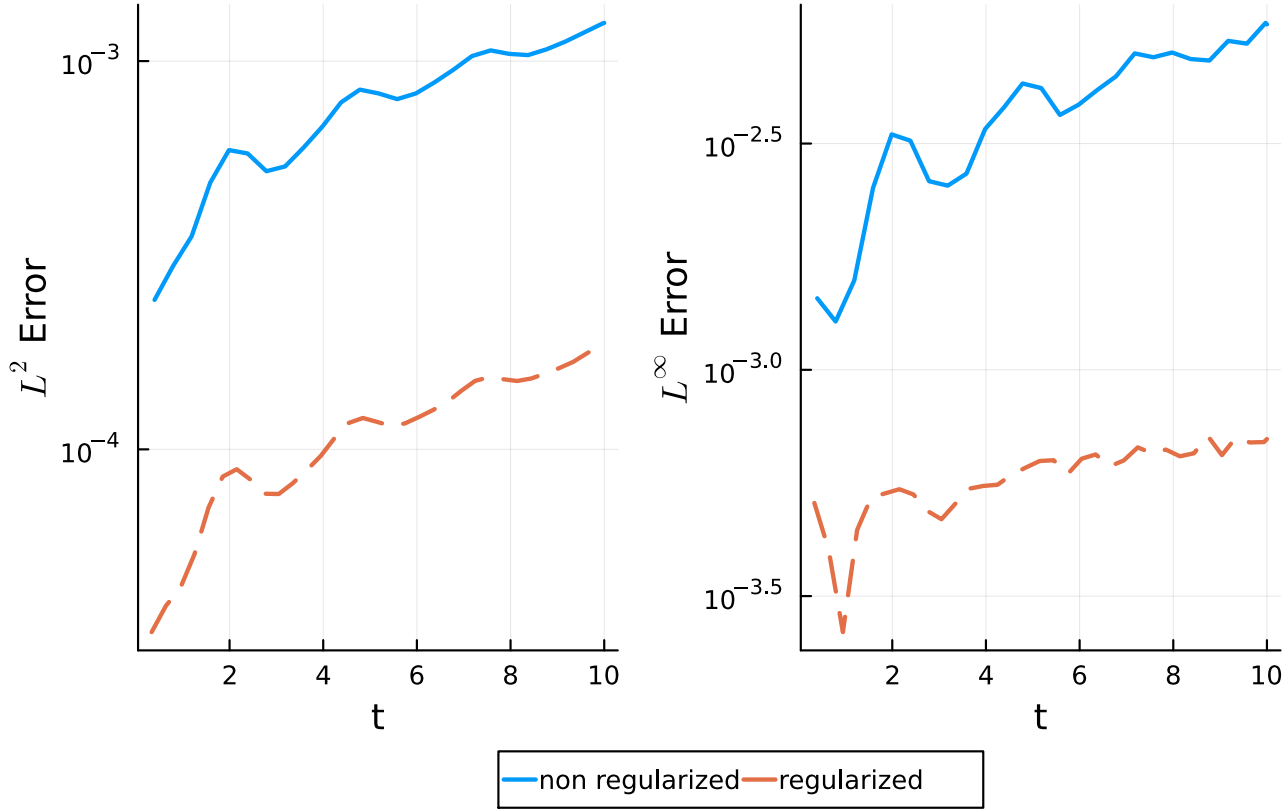


Figure 5: L^2 - and L^∞ -errors for the two-dimensional compressible Euler equations using FSBP operators based on $\mathcal{P}_3 = \text{span}\{1, x, x^2, x^3\}$ without regularization and with regularization on $\mathcal{G} = \{\sin(\pi x), \cos(\pi x)\}$ on 8 blocks with $N = 15$ nodes per block.

dimensional compressible Euler equations with manufactured solution (4.9) using FSBP operators based on $\mathcal{P}_3 = \text{span}\{1, x, x^2, x^3\}$ on 8 blocks with $N = 15$ equidistant nodes per block. We choose $\mathcal{G} = \{\sin(\pi x), \cos(\pi x)\}$ to promote accuracy on these modes and set $\lambda_1 = \lambda_2 = 1$. Note that the optimization without regularization does not converge for $\mathcal{P}_3 \cup \text{span}(\mathcal{G})$ to a residual of zero on the given set of nodes, suggesting that there does not exist an FSBP operator exact on this augmented basis. The L^2 - and L^∞ -errors are shown in Figure 4 and Figure 5. We observe that the regularized operators outperform the non-regularized ones. Again, the regularized operators are numerically nullspace consistent with rank $N - 1 = 14$, whereas the non-regularized ones have a rank of 8.

Remark 4.5. To solve the constrained optimization problem, we use the augmented Lagrangian method implemented in the Manopt.jl [4, 5] package.

5. Summary. We have demonstrated that fulfilling the formal definition of an SBP operator alone is not sufficient to guarantee accurate numerical solutions of hyperbolic conservation laws. By means of illustrative counterexamples, we showed that SBP operators may satisfy all standard algebraic conditions yet still exhibit poor approximation properties and convergence behavior. These deficiencies were traced to structural shortcomings—most notably, the existence of unresolved modes and the related lack of nullspace consistency.

To address these issues, we introduced two complementary strategies for improving the quality of SBP operators and introduced two variants of the optimization-based construction procedure for FSBP operators presented in [17]. First, we enforced sparsity in the differentiation matrix, which not only reduces computational cost and enables the usage of FSBP operators globally but also restores desirable numerical properties such as nullspace consistency and improved error behavior. Second, we discussed regularized optimization formulations that minimize the derivative error for higher-degree functions beyond the exactness space, thereby extending the accuracy of the constructed operators and diminishing unresolved modes.

Together, these results provide a clearer understanding of what additional structures are necessary for SBP operators to perform reliably in practice. The presented framework is general and applicable to arbitrary node distributions and function spaces, making it a flexible foundation for developing new high-order discretizations. Future work will focus on extending these results to meshfree methods for multi-dimensional problems, radial basis function SBP operators, and adaptive node distributions.

Acknowledgments. JG acknowledges support by the Swedish Research Council (VR) Starting Grant #2025-05370, the Zenith Career Development Grant #26.07, and the National Academic Infrastructure for Supercomputing in Sweden (NAIIS) grants #2025/22-1599 and #2024/22-1207. AI and JL acknowledge the support by the Deutsche Forschungsgemeinschaft (DFG) within the Research Training Group GRK 2583 “Modeling, Simulation and Optimization of Fluid Dynamic Applications”. PÖ is supported by the DFG within SPP 2410, project 525866748 and under the grant 520756621.

REFERENCES

- [1] R. ABGRALL, J. NORDSTRÖM, P. ÖFFNER, AND S. TOKAREVA, *Analysis of the SBP-SAT stabilization for finite element methods part I: Linear problems*, Journal of Scientific Computing, 85 (2020), pp. 1–29, <https://doi.org/10.1007/s10915-020-01349-z>.
- [2] R. ABGRALL, P. ÖFFNER, AND Y. LIU, *Some new properties of the PamPa scheme*, 2025, <https://arxiv.org/abs/2508.17147>.
- [3] W. BARSUKOW, C. KLINGENBERG, L. LECHNER, J. NORDSTRÖM, S. ORTLEB, AND H. RANOCHA, *Stability of the active flux method in the framework of summation-by-parts operators*, 2025, <https://arxiv.org/abs/2507.11068>.
- [4] R. BERGMANN, *Manopt.jl: Optimization on manifolds in Julia*, Journal of Open Source Software, 7 (2022), p. 3866, <https://doi.org/10.21105/joss.03866>.
- [5] R. BERGMANN, *Manopt.jl*, 2024, <https://doi.org/10.5281/zenodo.4290905>.
- [6] J. BEZANSON, A. EDELMAN, S. KARPINSKI, AND V. B. SHAH, *Julia: A fresh approach to numerical computing*, SIAM Review, 59 (2017), pp. 65–98, <https://doi.org/10.1137/141000671>.
- [7] M. H. CARPENTER, T. C. FISHER, E. J. NIELSEN, AND S. H. FRANKEL, *Entropy stable spectral collocation schemes for the Navier-Stokes equations: Discontinuous interfaces*, SIAM Journal on Scientific Computing, 36 (2014), pp. B835–B867, <https://doi.org/10.1137/130932193>.
- [8] J. CHAN, *On discretely entropy conservative and entropy stable discontinuous Galerkin methods*, Journal of Computational Physics, 362 (2018), pp. 346–374, <https://doi.org/10.1016/j.jcp.2018.02.033>.
- [9] D. C. DEL REY FERNÁNDEZ, J. E. HICKEN, AND D. W. ZINGG, *Review of summation-by-parts operators with simultaneous approximation terms for the numerical solution of partial differential equations*, Computers & Fluids, 95 (2014), pp. 171–196, <https://doi.org/10.1016/j.compfluid.2014.02.016>.
- [10] G. J. GASSNER, *A skew-symmetric discontinuous Galerkin spectral element discretization and its relation to SBP-SAT finite difference methods*, SIAM Journal on Scientific Computing, 35 (2013), pp. A1233–A1253, <https://doi.org/10.1137/120890144>.
- [11] J. GLAUBITZ, A. ISKE, J. LAMPERT, AND P. ÖFFNER, *Reproducibility repository for “Why summation by parts is not enough”*, https://github.com/JoshuaLampert/2026_SBP_not_enough, 2026, <https://doi.org/10.5281/zenodo.18596276>.
- [12] J. GLAUBITZ, S.-C. KLEIN, J. NORDSTRÖM, AND P. ÖFFNER, *Multi-dimensional summation-by-parts operators for general function spaces: Theory and construction*, Journal of Computational Physics, 491 (2023), p. 112370, <https://doi.org/10.1016/j.jcp.2023.112370>.
- [13] J. GLAUBITZ, S.-C. KLEIN, J. NORDSTRÖM, AND P. ÖFFNER, *Summation-by-parts operators for general function*

spaces: The second derivative, Journal of Computational Physics, 504 (2024), p. 112889, <https://doi.org/10.1016/j.jcp.2024.112889>.

[14] J. GLAUBITZ, J. LAMPERT, A. R. WINTERS, AND J. NORDSTRÖM, *Towards provable energy-stable overset grid methods using sub-cell summation-by-parts operators*, 2025, <https://arxiv.org/abs/2509.21442>.

[15] J. GLAUBITZ, J. NORDSTRÖM, AND P. ÖFFNER, *Summation-by-parts operators for general function spaces*, SIAM Journal on Numerical Analysis, 61 (2023), pp. 733–754, <https://doi.org/10.1137/22M1470141>.

[16] J. GLAUBITZ, J. NORDSTRÖM, AND P. ÖFFNER, *Energy-stable global radial basis function methods on summation-by-parts form*, Journal of Scientific Computing, 98 (2024), p. 30, <https://doi.org/10.1007/s10915-023-02427-8>.

[17] J. GLAUBITZ, J. NORDSTRÖM, AND P. ÖFFNER, *An optimization-based construction procedure for function space-based summation-by-parts operators on arbitrary grids*, Journal of Scientific Computing, 105 (2025), p. 83, <https://doi.org/10.1007/s10915-025-03062-1>.

[18] S. GOTTLIEB AND L.-A. J. GOTTLIEB, *Strong stability preserving properties of Runge–Kutta time discretization methods for linear constant coefficient operators*, Journal of Scientific Computing, 18 (2003), pp. 83–109, <https://doi.org/10.1023/A:1020338228736>.

[19] J. E. HICKEN, *Entropy-stable, high-order summation-by-parts discretizations without interface penalties*, Journal of Scientific Computing, 82 (2020), p. 50, <https://doi.org/10.1007/s10915-020-01154-8>.

[20] J. E. HICKEN, D. C. DEL REY FERNÁNDEZ, AND D. W. ZINGG, *Multidimensional summation-by-parts operators: General theory and application to simplex elements*, SIAM Journal on Scientific Computing, 38 (2016), pp. A1935–A1958, <https://doi.org/10.1137/15M1038360>.

[21] D. A. Kopriva, *Implementing Spectral Methods for Partial Differential Equations: Algorithms for Scientists and Engineers*, Scientific Computation, Springer Netherlands, Dordrecht, 2009, <https://doi.org/10.1007/978-90-481-2261-5>.

[22] H.-O. KREISS AND G. SCHERER, *Finite element and finite difference methods for hyperbolic partial differential equations*, in Mathematical Aspects of Finite Elements in Partial Differential Equations, C. de Boor, ed., New York, 1974, Academic Press, pp. 195–212, <https://doi.org/10.1016/B978-0-12-208350-1.50012-1>.

[23] V. LINDERS, *On an eigenvalue property of summation-by-parts operators*, Journal of Scientific Computing, 93 (2022), p. 82, <https://doi.org/10.1007/s10915-022-02042-z>.

[24] V. LINDERS, J. NORDSTRÖM, AND S. H. FRANKEL, *Properties of Runge–Kutta–summation-by-parts methods*, Journal of Computational Physics, 419 (2020), p. 109684, <https://doi.org/10.1016/j.jcp.2020.109684>.

[25] K. MATTSSON, M. ALMQUIST, AND M. H. CARPENTER, *Optimal diagonal-norm SBP operators*, Journal of Computational Physics, 264 (2014), pp. 91–111, <https://doi.org/10.1016/j.jcp.2013.12.041>.

[26] K. MATTSSON, M. ALMQUIST, AND E. VAN DER WEIDE, *Boundary optimized diagonal-norm SBP operators*, Journal of Computational Physics, 374 (2018), pp. 1261–1266, <https://doi.org/10.1016/j.jcp.2018.06.010>.

[27] K. MATTSSON AND J. NORDSTRÖM, *Summation by parts operators for finite difference approximations of second derivatives*, Journal of Computational Physics, 199 (2004), pp. 503–540, <https://doi.org/10.1016/j.jcp.2004.03.001>.

[28] P. K. MOGENSEN AND A. N. RISETH, *Optim: A mathematical optimization package for Julia*, Journal of Open Source Software, 3 (2018), p. 615, <https://doi.org/10.21105/joss.00615>.

[29] J. NORDSTRÖM AND M. BJÖRCK, *Finite volume approximations and strict stability for hyperbolic problems*, Applied Numerical Mathematics, 38 (2001), pp. 237–255, [https://doi.org/10.1016/S0168-9274\(01\)00027-7](https://doi.org/10.1016/S0168-9274(01)00027-7).

[30] J. NORDSTRÖM, K. FORSBERG, C. ADAMSSON, AND P. ELIASSON, *Finite volume methods, unstructured meshes and strict stability for hyperbolic problems*, Applied Numerical Mathematics, 45 (2003), pp. 453–473, [https://doi.org/10.1016/S0168-9274\(02\)00239-8](https://doi.org/10.1016/S0168-9274(02)00239-8).

[31] P. ÖFFNER, J. GLAUBITZ, AND H. RANOCHA, *Stability of correction procedure via reconstruction with summation-by-parts operators for Burgers’ equation using a polynomial chaos approach*, ESAIM: Mathematical Modelling and Numerical Analysis, 52 (2018), pp. 2215–2245, <https://doi.org/10.1051/m2an/2018072>.

[32] C. RACKAUCKAS AND Q. NIE, *DifferentialEquations.jl – a performant and feature-rich ecosystem for solving differential equations in Julia*, Journal of Open Research Software, 5 (2017), <https://doi.org/10.5334/jors.151>.

[33] H. RANOCHA, *Some notes on summation by parts time integration methods*, Results in Applied Mathematics, 1 (2019), p. 100004, <https://doi.org/10.1016/j.rinam.2019.100004>.

[34] H. RANOCHA, *SummationByPartsOperators.jl: A Julia library of provably stable semidiscretization techniques with mimetic properties*, Journal of Open Source Software, 6 (2021), p. 3454, <https://doi.org/10.21105/joss.03454>, <https://github.com/ranocha/SummationByPartsOperators.jl>.

[35] H. RANOCHA, P. ÖFFNER, AND T. SONAR, *Summation-by-parts operators for correction procedure via reconstruction*, Journal of Computational Physics, 311 (2016), pp. 299–328, <https://doi.org/10.1016/j.jcp.2016.02.009>.

[36] H. RANOCHA, M. SCHLOTTKE-LAKEMPER, A. R. WINTERS, E. FAULHABER, J. CHAN, AND G. GASSNER, *Adaptive numerical simulations with Trixi.jl: A case study of Julia for scientific computing*, Proceedings of the JuliaCon

Conferences, 1 (2022), p. 77, <https://doi.org/10.21105/jcon.00077>, <https://arxiv.org/abs/2108.06476>.

[37] M. SCHLOTTKE-LAKEMPER, G. J. GASSNER, H. RANOCHA, A. R. WINTERS, J. CHAN, AND A. RUEDA-RAMÍREZ, *Trixi.jl: Adaptive high-order numerical simulations of hyperbolic PDEs in Julia*. <https://github.com/trixi-framework/Trixi.jl>, 2025, <https://doi.org/10.5281/zenodo.3996439>.

[38] B. STRAND, *Summation by parts for finite difference approximations for d/dx* , Journal of Computational Physics, 110 (1994), pp. 47–67, <https://doi.org/10.1006/jcph.1994.1005>.

[39] M. SVÄRD AND J. NORDSTRÖM, *Review of summation-by-parts schemes for initial-boundary-value problems*, Journal of Computational Physics, 268 (2014), pp. 17–38, <https://doi.org/10.1016/j.jcp.2014.02.031>.

[40] M. SVÄRD AND J. NORDSTRÖM, *On the convergence rates of energy-stable finite-difference schemes*, Journal of Computational Physics, 397 (2019), p. 108819, <https://doi.org/10.1016/j.jcp.2019.07.018>.

[41] E. F. TORO, M. SPRUCE, AND W. SPEARES, *Restoration of the contact surface in the HLL-Riemann solver*, Shock Waves, 4 (1994), pp. 25–34, <https://doi.org/10.1007/BF01414629>.

[42] C. WILLIAMS AND K. DURU, *Full-spectrum dispersion relation preserving summation-by-parts operators*, SIAM Journal on Numerical Analysis, (2024), pp. 1565–1588, <https://doi.org/10.1137/23M1586471>.